On the Use of Plasmonic Nanoparticle Pairs As a Plasmon Ruler: The Dependence of the Near-Field Dipole Plasmon Coupling on Nanoparticle Size and Shape

ARTICLE *in* THE JOURNAL OF PHYSICAL CHEMISTRY A · MARCH 2009

Impact Factor: 2.69 · DOI: 10.1021/jp807904s · Source: PubMed

4 AUTHORS, INCLUDING:

Mahmoud A. Mahmoud
Georgia Institute of Technology
76 PUBLICATIONS **1,803** CITATIONS
SEE PROFILE

Mostafa A El-Sayed
Georgia Institute of Technology
675 PUBLICATIONS **54,814** CITATIONS
SEE PROFILE

On the Use of Plasmonic Nanoparticle Pairs As a Plasmon Ruler: The Dependence of the Near-Field Dipole Plasmon Coupling on Nanoparticle Size and Shape†

Christopher Tabor,‡ Raghunath Murali,§ Mahmoud Mahmoud,‡ and Mostafa A. El-Sayed*,‡

Laser Dynamics Laboratory and Microelectronics Research Center, Georgia Institute of Technology, Atlanta, Georgia 30332

Received: September 5, 2008; Revised Manuscript Received: October 29, 2008

The localized surface plasmon resonance (LSPR) spectral band of a gold or silver nanoparticle is observed to shift as a result of the near-field plasmonic field of another nanoparticle. The dependence of the observed shift on the interparticle distance is used as a ruler in biological systems and gave rise to a plasmonic ruler equation in which the fractional shift in the dipole resonance is found to decrease near exponentially with the interparticle separation in units of the particle size. The exponential decay length constant was observed to be consistent among a small range of nanoparticle sizes, shapes, and types of metal. The equation was derived from the observed results on disks and spherical nanoparticles and confirmed using results on a DNA conjugated nanosphere system. The aim of the present paper is to use electron beam lithography and DDA calculations to examine the constancy of the exponential decay length value in the plasmonic ruler equation on particle size and shape of a number of particles including nanoparticles of different symmetry and orientations. The results suggest that the exponent is almost independent of the size of the nanoparticle but very sensitive to the shape. A discussion of the nanoparticles most suitable for different applications in biological systems and a comparison of the plasmonic ruler with Forster resonance energy transfer (FRET) is mentioned.

Introduction

Metallic nanoparticles are of great interest due to their optical and radiative properties. The interaction of a noble metal nanoparticle with incident light of a specific energy induces intense localized fields at the surface of the particle. These fields are induced when conduction band electrons of the noble metal nanoparticle couple with the electric field of incident light at a resonant frequency, generating a plasmonic oscillation localized on the surface of the nanoparticle, known as the localized surface plasmon resonance (LSPR).[1−4] This plasmonic oscillation occurs at a specific resonance wavelength that is dependent on the particle's properties (dielectric function, size, and shape) and the dielectric constant of the host medium. By changing these parameters, one can tune the optical properties of the noble metal nanoparticles to optimize them for different applications. The intense localized field at the nanoparticle surface and the tunability of the LSPR in noble metal nanoparticles gives them enormous potential in medical,[5−7] optical,[8−11] and sensor[12−16] applications.

When two nanoparticles come into close contact (separations of less than 2 particle diameters), the near-field dipole plasmonic fields couple with one another, reducing the overall resonance energy of the particle pair.[17−19] Colloidal studies have provided initial qualitative data on the near-field coupling between plasmonic nanoparticles, and many groups[12,20,21] have reported on the effect of aggregation on the optical extinction of nanoparticles in solution. To achieve quantitative measurements of the coupling of two plasmonic metal nanoparticles, it is necessary to use lithographic techniques to fabricate nanoparticles of homogeneous size, shape, and interparticle separation. However, only recently has it been technologically possible to fabricate nanoparticles of high homogeneity and low feature size thanks to advancements in electron beam lithography (EBL).

Quantitative studies on the near field dipole plasmon coupling between two nanoparticles as a function of interparticle separation were independently first reported by Su et al.[22] and Rechberger et al.[17] in a spheroidal gold nanoparticle. They concluded that "when the [LSPR] peak shift is scaled by the peak wavelength and the gap is scaled by the particle... length, all data points fall on a *common curve*." The common curve was an exponential decay of the coupling, measured by the fractional shift in the plasmon resonance ($\Delta\lambda/\lambda$), as a function of the interparticle separation (s) scaled by the particle size (D). It was later shown that while the true dependence of the dipole coupling on the scaled interparticle separation goes as $(s/D)^{-3}$, a single exponential of the form $(\Delta\lambda/\lambda) = A \times e^{(-s/D/\tau)}$ very nearly approximates the dependence.[23] This exponential approximation is also useful for quantifying the relative strength of the dipole field by the magnitude of the pre-exponential factor A and the decay length of the field away from the particle surface by the magnitude of τ.

Using discrete dipole approximation (DDA) calculations, our group has examined the plasmonic decay law for nanospheres,[23,24] nanoshells,[25,26] nanoellipses,[24] and nanodisks,[23] and using electron beam lithography (EBL) the gold nanodisk was studied and the exponential decay length value was found to agree with the DDA results and with the results of silver nanodisks.[27] From these studies it was concluded that this common coupling trend has a scaled decay length that is largely independent of the particle material, dielectric environment, size, and shape.[23−26] We have also loosely shown mathematically why this decay of the scaled quantities should be largely independent of the nanoparticle properties.[23] By using this common coupling behavior a plasmon ruler equation was developed. Work from

* Corresponding author. E-mail: melsayed@gatech.edu.
† Part of the "Max Wolfsberg Festschrift".
‡ Laser Dynamics Laboratory, Georgia Institute of Technology.
§ Microelectronics Research Center, Georgia Institute of Technology.

10.1021/jp807904s CCC: $40.75
Published on Web 12/17/2008

Reinhard et al.[21] demonstrated experimentally controlled separation of two 40 nm nanospheres in solution by using conjugated DNA. Accurate control over the nanosphere separation was obtained by conjugating one colloidal solution with a single strand of DNA and conjugating a second colloidal solution with the complimentary single strand of DNA. When the two colloidal solutions were mixed, the resulting DNA hybridization formed a rigid molecular spacer between two nanospheres of a well-defined length. Jain et al. applied the developed plasmon ruler to this system and calculated the interparticle separation accurately using only the optical extinction of the particles.[23] This plasmonic ruler technique possesses advantages over the traditionally used FRET (Forster resonance energy transfer) technique, which uses fluorescent quenching between two reporter dye molecules to optically determine the molecular separation. The quenching has a $1/R^6$ dependence on the separation distance, whereas the distance dependence of plasmonic coupling occurs as $1/R^3$, which affords the plasmonic ruler a larger range of measurement, on the order of 1−100 nm (1−10 nm in FRET[28,29]). Additionally, absorption and scattering processes are used to detect the plasmonic particle separation, which is advantageous over fluorescence emission because the signal does not photobleach like the FRET signal does.[21]

While these conclusions were made based on extensive simulated data using well-established DDA calculations and several experimental systems, these systems were generally isosymmetric, most particles having at least one C_∞ axis of symmetry and all particles possessing a center of inversion. The symmetrical similarities of the shapes that have been studied thus far (nanospheres, nanodisks, nanoellipses, and nanoshells) have neglected to truly investigate the "independent" nature of the exponential decay length. Moerner et al.[30] have reported on the coupling between two nanoprisms oriented tip-to-tip ("bowtie" particles) fabricated on silicon using EBL. A similar qualitative exponential decay in the plasmonic coupling was observed as the tip-to-tip separation was increased. Finite-difference time-domain (FDTD) calculations were preformed and a good agreement was reported between the simulated and the experimental data points.

In the present report, we show experimentally that the quantitative decay of the dipole plasmon coupling between two nanoparticles is dependent on the nanoparticle shape, but is generally not highly sensitive to nanoparticle size. We reexamine previous reports on the existence of a universal constant that governs the near exponential decay of the coupling between the surface plasmons of two nanoparticles. While there is no universal decay constant for all nanoparticle shapes, the exponential decay length and amplitude that express the dipole coupling can often be approximated as constants over a range of sizes for a given shape.

Experimental Methods and Theoretical Simulations

Nanoprism arrays were fabricated using a JEOL JBX-9300FS 100 kV electron beam lithography (EBL) system. The substrates used to support the nanoprisms were prefabricated free-standing silicon nitride membranes whose fabrication has been described in detail elsewhere.[31] Briefly, silicon wafers with a ⟨100⟩ orientation were purchased from University Wafer and cleaned and placed in a Tystar Furnace. Si_3N_4 was deposited onto the wafer surface using a low-pressure chemical vapor deposition process at a deposition rate of 5 nm/min to a final thickness of 50 ± 3 nm. A combination of optical photolithography and dry etching with CF_4 removed selected areas of the membrane from one side of the wafer. These areas were exposed to KOH to anisotropically etch the silicon wafer through to the other side, exposing the other silicon nitride membrane. This produced an array of silicon nitride membrane windows freely supported that were $150 \times 150\ \mu m^2$. Each window was used for a single design pattern and each pattern array was $300 \times 300\ \mu m^2$ in order to ensure pattern overlap with the window. A poly methyl methacrylate (PMMA) positive electron resist was spin coated onto the top Si_3N_4 side of the wafer to a thickness of 80 nm. A dose of 2750 $\mu C/cm^2$ was used to write the pattern at a beam current of 1.98 nA. Development of the exposed areas was carried out in a 1:3 methyl isobutyl ketone: isopropyl alcohol (MIBK:IPA) solution for 10 s. The sample was then washed in IPA for 30 s before gently drying in a stream of N_2. A thin chrome layer (0.5 nm at 0.1 A/s) was evaporated onto the sample using a CVC electron beam evaporator followed by a 20.0 nm layer of gold at a rate of 0.5 A/s. The Cr served as an adhesion layer between the Si_3N_4 surface and the Au nanoparticles. Final lift-off and removal of the PMMA mask was accomplished by placing the sample in 1165 remover purchased from MicroChem for 24 h. The array was designed so that the nanoparticle dimer pairs were spaced more than 800 nm from one another to reduce far-field coupling that has been observed by Rechberger et al.[17] in 150 nm diameter gold nanodisk arrays. This far-field coupling has been shown by the Moerner group to exist at large separations (4−7 prism bisector separations) for tip-to-tip nanoprisms. For this reason, individual particle pairs were experimentally spaced no less than 8 particle diameters apart and no interparticle separations were used greater than 3 particle bisectors. In these experimental samples with small interparticle gaps (15−200 nm), the near-field coupling can be expected to be much stronger than any far-field grating effects.

The supported nanoprisms were imaged using a Zeiss Ultra60 Scanning Electron Microscope (SEM). Absorption measurements were done on a Craic 1100 microabsorption spectrophotometer in transmission mode under polarized light using a 20x magnification. The collection spot was $\sim 8.0 \times 8.0\ \mu m^2$ and several different areas were collected from the center of the array and averaged to produce the reported spectra. A comparison between magnified SEM images from various membrane windows show excellent homogeneity in the particle shapes as the spacing is increased from 15 to 200 nm.

The optical response of the nanoparticle shapes have been calculated using the DDA method with the DDSCAT 6.1 code publicly offered by Draine and Flatua[32] and modified by Goodman.[33] The method has been described in great detail elsewhere.[1] Briefly, the method approximates the desired particle shape as a 3-dimensional cubic lattice of polarizable point dipoles of preprogrammed dipole−dipole spacing. The program solves for the scattering and absorption of each polarizable point self-consistently in response to an incident plane polarized wave light and polarization of neighboring dipole points. The bulk values of the dielectric constants reported by Johnson and Christy[34] for gold were used. The DDA method has been demonstrated by many groups[35−38] to be suitable for optical calculations of the extinction spectrum and the local electric field distribution in metal particles with different geometries and environments. The incident light is always polarized parallel with the interparticle axis in this report and the dielectric of the host medium was set at $\varepsilon_m = 1.00$. As discussed by Rechberger et al.,[17] it is reasonable to consider in the calculations of a single particle pair instead of the entire 2-D array. This consideration is justifiable because the particle pairs in the experiment are separated from each other by large distances on the order of 8

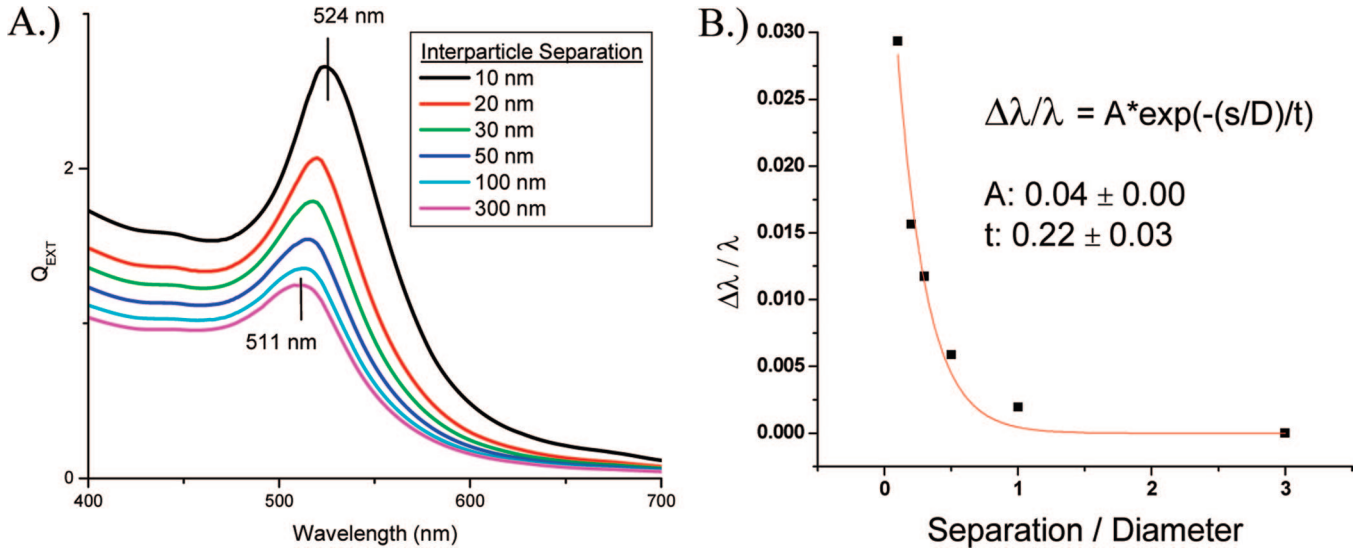

Figure 1. (A) DDA simulation of the optical extinction of two nanospheres (D=40 nm) at various interparticle separations. (B) The dipole plasmon coupling of two nanospheres measured as the fractional shift in the plasmon resonance ($\Delta\lambda/\lambda$) plotted as a function of the interparticle separation scaled by the diameter of the nanosphere. The red line is a single exponential decay best-fit to the data (with a correlation coefficient of R^2=0.98) of the form $y = A \times \exp(-x/t)$. The values for the amplitude (A) and decay (t) are 0.04 and 0.22, respectively.

particle diameters, large enough so that no coupling occurs between different particle pairs. This ensures that only the interactions between the two particles within the dimer are measured.

Results

I. Nanosphere. We begin with DDA calculations on the nanosphere, since it is the easiest gold nanoparticle shape to synthesize and has been previously utilized in numerous applications, including the plasmon ruler equation. This application fundamentally requires a well-developed understanding of the coupling between two nanospheres and knowledge of how the plasmon resonance of the particle pair depends on the interparticle separation. DDA calculations were preformed on simulations of two identical gold nanospheres with diameters throughout the range $5 > D > 50$ nm at various interparticle separations. For each nanosphere size, the plasmon dipole resonance was calculated for 6 various interparticle separations. Representative calculated spectra are shown in Figure 1A. Each separation results in a unique SPR extinction maximum. The fractional shift of the SPR maximum wavelength ($\Delta\lambda/\lambda$) is plotted as a function of the interparticle separation (s) scaled by the diameter of the nanoparticle (D), shown in Figure 1B. Additional spectra and dipole coupling fits can be found in the Supporting Information.

This dependence has previously been explored[23] and mathematically found to obey the dependence

$$\frac{\Delta\lambda}{\lambda}(s/D) = \frac{1}{(12\Lambda(s/D+1)^3 - (1+\gamma))} \quad (1)$$

where both $\gamma$and Λ are variables relating the shape and size of the nanoparticle. This dependence is very closely approximated as a single exponential decay of the following form:

$$\frac{\Delta\lambda}{\lambda} = A \times e^{\left(\frac{-s/D}{t}\right)} \quad (2)$$

It is this exponential approximation that led to the formulation of the plasmon ruler equation,[23] where $A = 0.18$ and $t = 0.23$, which was successfully used to measure separations of nanosphere particles in solution using their optical extinction. Table 1 lists the decay values and amplitudes of the best-fit exponential decay approximation for a range of nanosphere sizes calculated using the DDA method. The decay values are plotted in Figure 2 as a function of the nanosphere volume. Over this size range ($5 > D > 50$ nm) the decay value has a negligible dependence on the size of the nanosphere. The plasmon ruler equation is not greatly affected by the weak dependence of these fitting values on the nanosphere size when the size is $D < 50$ nm. The exponential decay length previously reported ($t = 0.23$) is the average value over this range. While this decay length does not significantly vary at small sizes ($D < 50$ nm), caution is recommended when using nanospheres larger than 50 nm in diameter since the deviation in the plasmon coupling could become significant.

TABLE 1: Au Nanospheres (DDA)

diameter (nm)	amplitude[a]	decay length[a]
5.0	0.039 ± 0.004	0.25 ± 0.03
10.0	0.038 ± 0.003	0.24 ± 0.02
20.0	0.042 ± 0.006	0.22 ± 0.04
30.0	0.040 ± 0.003	0.24 ± 0.02
40.0	0.045 ± 0.004	0.22 ± 0.03
50.0	0.045 ± 0.004	0.21 ± 0.03

[a] $\varepsilon_m = 1.00$ (air).

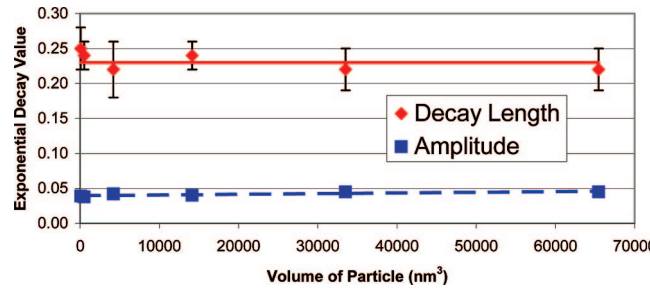

Figure 2. Variation in the plasmon coupling decay length (t) and amplitude (A) of two gold nanospheres as a function of the nanosphere volume. Variation in both values as a function of volume is negligible within error.

II. Nanodisks. Previously we have referred to the decay of the dipole plasmon coupling between particles as "universal", being independent of the particle's size and shape. This conclusion

TABLE 2: Au Nanodisk (DDA)

diameter (nm)	thickness (nm)	amplitude[a]	decay length[a]
100.0	20.0	0.17 ± 0.01	0.28 ± 0.03
75.0	15.0	0.13 ± 0.01	0.24 ± 0.03
50.0	10.0	0.11 ± 0.01	0.23 ± 0.03
30.0	6.0	0.10 ± 0.01	0.22 ± 0.03
20.0	4.0	0.10 ± 0.01	0.21 ± 0.02
10.0	2.0	0.09 ± 0.01	0.21 ± 0.02
100.0	10.0	0.14 ± 0.01	0.33 ± 0.04
100.0	14.0	0.16 ± 0.02	0.30 ± 0.05
100.0	20.0	0.17 ± 0.01	0.28 ± 0.03
100.0	24.0	0.17 ± 0.02	0.27 ± 0.03
100.0	30.0	0.18 ± 0.02	0.26 ± 0.04

[a] $\varepsilon_m = 1.00$ (air).

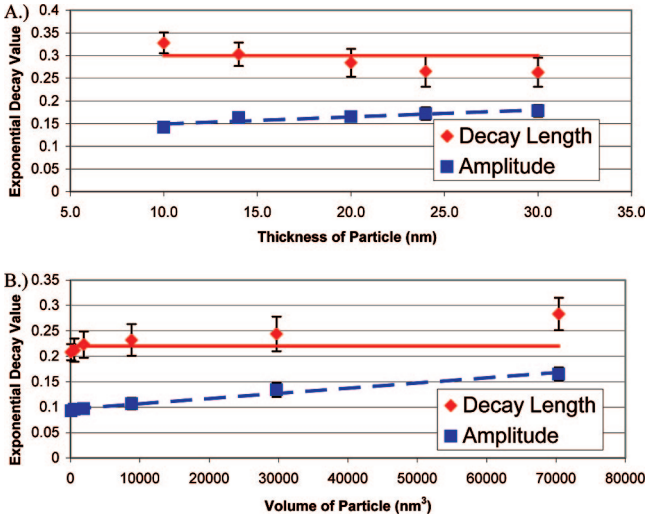

Figure 3. (A) The dependence of the decay length (red diamonds) and amplitude (blue squares) of the dipole plasmon coupling between two nanodisks as a function of nanodisk thickness. The diameter is held constant at 100 nm. (B) The dependence of the decay length (red diamonds) and amplitude (blue squares) of the dipole plasmon coupling between two nanodisks as a function of nanodisk volume. The aspect ratio of the disks (D/T) is held constant at 5.

was largely based on similarities in the value of the best-fit exponential decay for other shapes in addition to nanospheres, specifically nanodisks,[23] which were experimentally and theoretically determined. Here we have varied the dimensions of the nanodisk and computed the influence of the dimensions of the disk (thickness, volume) on the dipole plasmon resonance coupling. Table 2 displays various nanodisk dimensions and the respective decay values and amplitudes associated with them.

The exponential values listed in Table 2 for nanodisk pairs are plotted in Figure 3. Variation in the nanodisk volume has a negligible effect on the nanodisk dipole coupling constants until the nanodisk diameter exceeds 75 nm. When the diameter of the nanodisk becomes large (100 nm) the decay constants slightly increase. As the thickness of the nanodisk is varied, there is also a negligible deviation in the exponential decay coupling values. It is worth noting that while the dependence of the dipole plasmonic decay values on the nanoparticle volume is extremely weak, there can be significant variation in the values when the nanodisk dimensions or aspect ratio (diameter/thickness) are excessively varied. The average exponential decay length for a nanodisk of an aspect ratio of 5 is 0.22 ± 0.02 (Figure 3A) while the average exponential decay length of a large nanodisk ($D = 100$ nm) averaged over several different aspect ratios is 0.30 ± 0.02 (Figure 3B). These significant variations are attributed to an extreme change in the nanodisk

TABLE 3: Au Nanoprism (DDA)

bisector (nm)	base (nm)	thickness (nm)	amplitude[a]	decay length[a]
69.4	81.0	19.8	0.11 ± 0.01	0.36 ± 0.05
57.1	66.6	16.3	0.10 ± 0.01	0.35 ± 0.04
38.1	44.4	13.0	0.09 ± 0.01	0.33 ± 0.02
17.3	20.2	5.9	0.09 ± 0.01	0.30 ± 0.03

[a] $\varepsilon_m = 1.00$ (air).

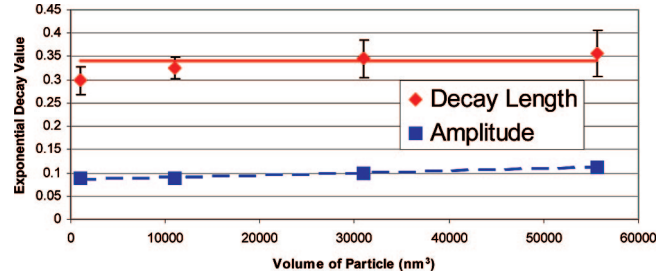

Figure 4. Dependence of the decay length (red diamonds) and amplitude (blue squares) of the dipole plasmon coupling between two nanoprisms as a function of nanoprism volume. The aspect ratio of the prisms (bisector/thickness) is held constant at 3.5. The "average" line drawn over the decay length data (red) includes the experimental data.

dimensions (shape), which has a significant effect on the strength of the induced plasmonic field.[39] However, within a reasonable size range (diameter = 10−75 nm), the effects of the size on the nanodisk exponential coupling of a set aspect ratio and particle shape are negligible.

It is worth noting that the experimental value for the decay length previously found for gold nanodisks of diameter $D =$ 88 nm and thickness $T = 25$ nm was 0.18 ± 0.02 and does not match the values reported here. We believe that this value does not fall within the range found in Table 2 because there are only a few data points provided to obtain the data experimentally,[23] and none of the points fall around $s/D = 1$ where the greatest deviation occurs between the exponential fit and the true x^{-3} dependence. Experimental data points in this region should result in a slightly larger best-fit single exponential decay length, consistent with our findings here.

III. Nanoprisms. We now move on to discuss the prismatic shaped nanoparticle and the effect of dimensional changes on the decay of the coupling between two nanoprisms oriented tip-to-tip. This dimer system is of interest to the field of molecular sensing due to predicted high fields at the nanoprism tip upon excitation at the surface plasmon resonance frequency.[39] This intense field is the foundation of surface enhanced spectroscopies on metallic surfaces, which have gained enormous attention recently.[14,40,41] Specifically, the enhancement factor for a surface enhanced Raman scattered photon is proportional to the enhancement of the field to the fourth power. The nanoprism is also of interest to the discussion here because of its unique symmetry compared with the other nanoparticle shapes studied, lacking a center of inversion.

The optical extinction for several equilateral nanoprism dimers of various volumes were theoretically computed using the DDA method. Table 3 lists the decay length and amplitude values of the best-fit single exponential curves fit to the fractional shift in the plasmon resonance wavelength as a function of scaled interparticle separation for various equilateral nanoprisms. The coupling values are plotted in Figure 4 as a function of the total volume.

Similar to the nanodisk, there is a negligible increase in both coupling constants as the total volume of the nanoprism is

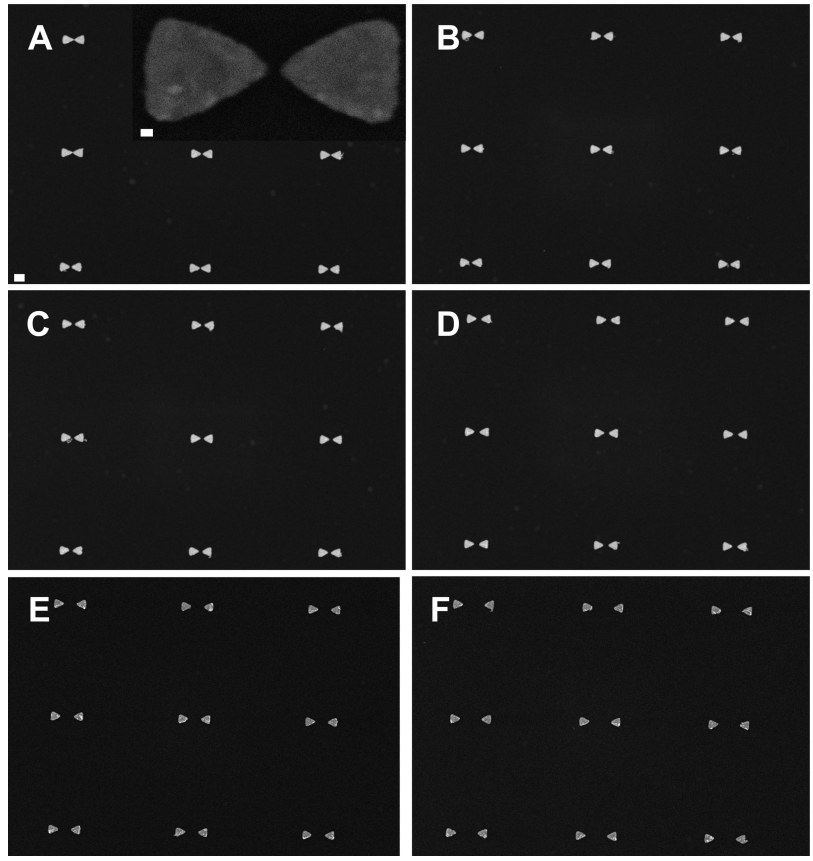

Figure 5. Nanoprism dimers fabricated by EBL with increasing interparticle separation 14.4, 23.1, 30.2, 34.7, 124.8, and 202.1 nm separation for A−F, respectively. The inset in part A is one of many highly magnified SEM images that were used to take statistical measurements of the particle dimensions.

TABLE 4: Au Nanoprisms (Experimental)

bisector (nm)	base (nm)	side (nm)	thickness (nm)	amplitude	decay length
87.0 ± 3.6	79.7 ± 2.8	89.2 ± 3.8	20 ± 1	0.13 ± 0.01	0.34 ± 0.02
83.0 ± 5.1	72.2 ± 2.7	81.4 ± 4.1	20 ± 1	0.12 ± 0.01	0.36 ± 0.02

increased. This is again due to higher order multipoles strengthening the dipole plasmon fields during plasmonic coupling. The interesting result here is that the average decay length is much higher for nanoprisms (0.33) than it is for either the nanodisks (0.22) or the nanospheres (0.23). Physically, this result indicates that the surface field extends further out from the particle in nanoprisms than in nanodisks and nanospheres, quantitatively 50% further. This phenomenon is due to high field intensities at the surfaces of nanoprisms due to the high curvature tip region.

These DDA simulations are compared to experimental nanoprism dimers of various separations fabricated by EBL. We have fabricated a near equilateral nanoprism shape that possesses some of the most extreme dimensions of this study, which results in the more extreme coupling values. Nanoprisms with large volumes and low aspect ratios (bisector/thickness) were used for this purpose. Scanning electron microscopy (SEM) images of the nanoprism dimers fabricated by electron beam lithography (EBL) are shown in Figure 5. Statistical analyses of the nanoprism dimensions were taken for more than 200 particles at the center of each array, in the same location where the optical spectra were taken. The average dimensions of two samples are given in Table 4. The radius of curvature for the nanoprisms was roughly 10 nm.

Figure 6A shows the unaltered microabsorption spectra of several nanoprism dimers from 200 to 14 nm interparticle separations. The irradiation light was polarized parallel to the interparticle axis for all spectra. The large decrease in intensity for the closest particles (14.4 nm separation) is due to some particle pairs fusing together at these shortest separations. When fusing occurs to form one large particle the optical extinction maximum shifts far to the red, outside of the field of analysis, and therefore does not affect the plasmon band position of the separated particles. For the least separated nanoprisms, the separation gap was 14.4 ± 3.9 nm. These measurements did not include the fused particle pairs with a gap = 0 nm. For all other arrays of particle separations the error for the reported interparticle separation was less than 3.9 nm. Figure 6B shows the experimental relationship between the coupling of the dipole plasmon resonance of the nanoprisms, monitored by the fractional shift in the plasmon resonance ($\Delta\lambda/\lambda$), as a function of the interparticle separation scaled by the nanoprism size. The experimental data is fit to a single exponential decay. We find that the exponential fit is a good approximation for nanoprism particles, evidenced by the high R^2 fitting of 0.98. We report for the first time experimental evidence of the nonuniversality of the coupling decay constant seen in so many previous cases with more symmetric nanoparticle systems, which have a value between $0.18 \leq t \leq 0.23 \pm 0.04$. It is clear that the experimental data for nanoprisms does not fit this exponential decay value but decays with a value roughly 50% higher ($t = 0.35 \pm 0.02$), as predicted by the DDA calculations.

The size of the nanoprism is defined by the prism bisector, which is used to scale the interparticle separation. It is beneficial to discuss the appropriateness of using the nanoprism bisector to describe the size. For all nanoparticles investigated in this way to date, the size of the particle has been intuitively defined

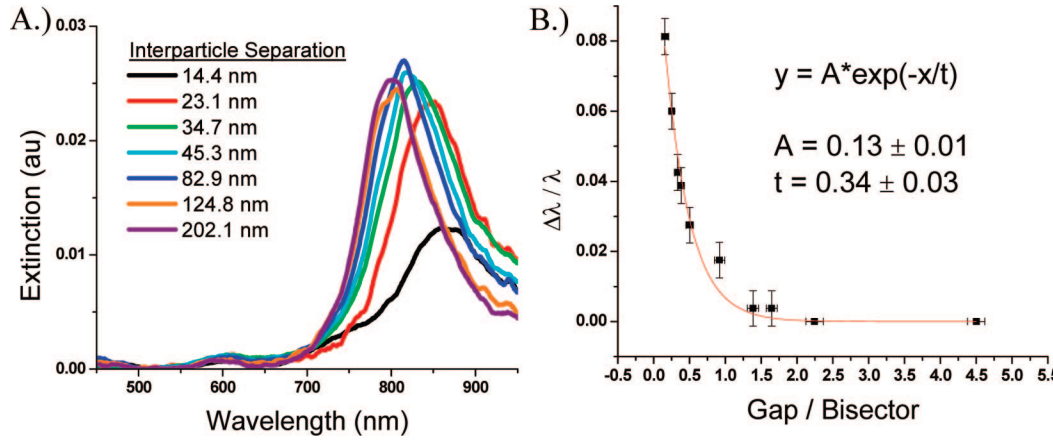

Figure 6. (A) Experimental extinction spectra of selected nanoprism dimer pairs with various tip-to-tip interparticle separations. (B) Experimental results of the dipolar plasmon resonance coupling ($\Delta\lambda/\lambda$) between two nanoprisms oriented tip-to-tip as a function of the interparticle separation scaled by the particle size.

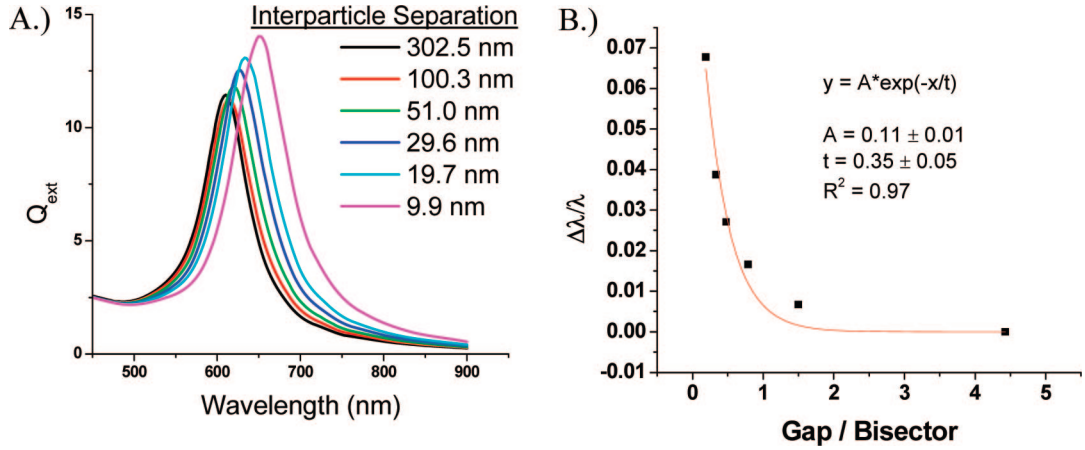

Figure 7. (A) DDA simulation of two nanoprism particles oriented tip-to-tip with various interparticle separations. Nanoprism dimensions match those of the experimental samples. (B) Single exponential best-fit curve demonstrating the theoretical relationship between the fractional dipole plasmon shift as a function of the scaled interparticle separation. Black squares are the data points obtained from DDA calculations.

as the length of the particle along the interparticle axis. For example, the size of a nanodisk is defined as the diameter of the disk. The loss in inversion symmetry for nanoprisms requires that we justify the use of the bisector, since the plasmon oscillation occurs as two dipoles along each of the nanoprism sides, which has been both theoretically[1,42] and experimentally[39] determined when the polarization of the light is parallel to the nanoprism bisector, as is true in our case. This unique situation is not observed for the higher symmetry nanoparticles such as disks, spheres, and shells. Even the nanoellipses studied by Su et al.[22] possess only one established dipole that is parallel to both the interparticle axis and the incident polarization of light. Although the induced dipoles in the nanoprism are not oriented parallel to the interparticle axis, the net summation of the vectors is along that axis and is the reason that the resonance coupling between the electrons of the metal nanoparticle and the electric field of the light occurs.

The optical extinction spectra for similar sized nanoprisms are simulated in Figure 7A and the dipole plasmon coupling dependence on the interparticle separation is plotted in Figure 7B. The blue shift in simulated spectra compared with the experimental spectra is likely due to the dielectric constant surrounding the nanoprisms. The experimental nanoprisms are supported on a silicon nitride substrate in ambient conditions, while the theoretical calculations assumed an environmental dielectric constant equal to that of air. While this has a great effect on the absolute plasmon resonant energies, the decay length and amplitude of the dipole plasmon coupling is nearly identical in the experimental and theoretical work.

We also observed in all theoretical calculations and experimental spectra a strong deviation from the exponential approximation when the interparticle separation is equal to the nanoparticle size, ($S/D \approx 1$). This deviation is very pronounced in the experimental work, as can be seen in Figure 6, where the error bars for the data point $S/D \approx 1$ do not overlap the single exponential best-fit. This deviation was also observed for other theoretical studies for various particle shapes,[23,24,26] but this is the first reported experimental confirmation of that deviation. It has previously been explained as a deviation of the exponential approximation from the true cubic equation, derived elsewhere.[23] Caution is given when using the plasmonic ruler equation in the region of $S/D \approx 1$ due to the large deviation from the exponential approximation.

IV. Nanocubes. To emphasize the effect that intensified surface fields have on the dipole plasmon coupling between two nanoparticles, we have investigated the effect of size on the exponential coupling between two gold nanocubes. The fractional shift in the dipole plasmon wavelength was plotted as a function of the interparticle separation scaled by the edge length of the nanocube when the nanocube sides are facing one another. The exponential decay values for the best-fit single exponential for various nanocube volumes are given in Table 5 and plotted in Figure 8 as a function of nanocube edge length. Similar to

TABLE 5: Au Nanocube (DDA)

edge length (nm)	volume (nm^3)	amplitude[a]	decay length[a]
10	1000	0.05 ± 0.01	0.35 ± 0.02
20	8000	0.05 ± 0.01	0.35 ± 0.02
30	27000	0.06 ± 0.01	0.39 ± 0.03
40	64000	0.07 ± 0.01	0.41 ± 0.04
50	125000	0.10 ± 0.01	0.38 ± 0.04

[a] $\varepsilon_m = 1.00$ (air).

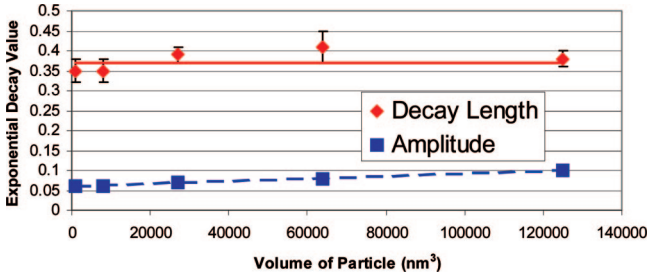

Figure 8. Dependence of the decay length (red diamonds) and amplitude (blue squares) of the dipole plasmon coupling between two nanocubes oriented side to side as a function of nanocube volume.

TABLE 6

nanoparticle shape	decay length (t)
gold nanosphere	0.23 ± 0.03
gold nanodisk (Dia/Th = 5)	0.22 ± 0.03
gold nanoprism (tip-to-tip)	0.35 ± 0.03
gold nanocube (side to side)	0.37 ± 0.03

other shapes explored here, the size of the nanocube has a negligible effect on the decay length of the dipole plasmon coupling.

Like nanoprisms, the nanocube has regions of high curvature and it has been shown through electrodynamic calculations that the rectangular shape possesses strong fields around these high curvature areas,[43] more intense than a nanoprism. These intense fields lead to an even higher dipole plasmonic coupling decay length (0.37), larger than the nanoprism (Table 6).

V. Practical Applications of Nanoparticles as a Plasmon Ruler. As a concluding discussion, we would like to point out that for general applications of the nanoparticle plasmon ruler the ideal nanoparticle size and shape selection should be a small nanosphere ($D < 50$ nm). The exponential decay constants used to approximate the dipole plasmon coupling of nanospheres in this size regime have a negligible dependence on the nanoparticle size, thus errors due to the dispersion in size will be minimized. Gold nanospheres are one of the easiest nanoparticles to homogeneously synthesize, making them practically preferable to other colloidal nanoparticle shapes. Smaller nanoparticles are preferred in biological systems because the structural perturbation of the biological system caused by the conjugated nanoparticles will be minimized.

For completion, it is important to discuss the advantages and disadvantages that the plasmonic ruler possesses compared to the traditionally used FRET technique. As mentioned in the introduction, FRET performs accurately in measuring intersite distances of 1−10 nm[28,29] while the nanoparticle plasmonic ruler operates on a much wider range of 5−100 nm depending on the nanoparticle size and shape.[23] The two techniques are complimentary to one another in this respect. However, the advantage of single molecule FRET is that the optical reporter is very small in size (molecular) and has a minimal perturbation effect on the structure of the system. Metallic nanoparticles used in the plasmonic ruler technique are much larger than the molecular size used in their FRET counterparts.

While nanospheres generally will be the choice of particle shape in the plasmon ruler applications, the results here demonstrate that less symmetrical particle shapes with high curvature features such as tips and corners can increase the plasmonic coupling range. Particularly the large value of the decay length of the dipole plasmon coupling between nanoprisms oriented tip-to-tip and nanocubes oriented side to side ($t \sim 0.37$) compared to nanospheres or nanodisks ($t \sim 0.23$) suggests that the probe range of nanoprisms is roughly 50% larger. This allows one to obtain the same measurement for smaller nanoprisms that would only be possible using larger nanospheres. For biological samples the smaller the nanoparticle antennas are that perform the measurement the less perturbation is introduced to its structure, and for this reason the prismatic or cubic shape would be preferred, as long as orientational dependence of the particles relative to one another is understood. Presently, a biologist using nanospheres does not need to concern themselves with orientation effects of the two spheres relative to one another. However, future studies are centered on investigating the orientational dependence of the exponential constants in low symmetry nanoparticles and nanoparticle systems to allow the nanoparticles to function not only as a 1-dimensional ruler but also as a 2 or 3-dimensional mapping agent for biological systems.

Summary

We have found experimental evidence and computational support of the shape dependence of the dipole plasmon coupling on distance between pairs of gold nanoparticles. This coupling has been quantitatively described by the fitting parameters of a best-fit single exponential decay of the fractional shift in the wavelength of the dipole surface plasmon resonance of the particle pair as a function of the interparticle separation scaled by the nanoparticle size. The two fitting parameters are the amplitude and the decay length. The amplitude physically describes the maximum fractional shift, which occurs at zero separation of the pair and is proportional to the maximum value of the overlapping field strength of the two particles. The decay length is the length over which the combined field decays as the pair moves away from one another. From these results, we conclude that nanospheres below $D = 50$ are generally the most practical nanoparticle shape to use as a plasmonic ruler. Other nanoparticle shapes of stronger plasmonic fields (such as nanocubes and nanoprisms) can be used to extend the measurement to longer intersight binding separations. However, orientational control over these less symmetric particles must be understood, since variations in the particle orientations can likely result in changes in the exponential plasmonic coupling decay length. Work is currently being carried out to better understand the dependence of the exponential decay length on the particle orientations.

Acknowledgment. This work was supported by the Materials Research Division of the National Science Foundation (No. 0527297). We thank B. T. Draine and P. J. Flatau for use of their DDA code, DDSCAT 6.1 and Cheng-Tsung Lee for supplying the Si_3N_4 substrates. The DDA simulations were completed using the computing facilities at the Center for Computational Molecular Science and Technology (CCMST).

Supporting Information Available: Supplementary Figure 1, DDA simulations of the optical extinction of four representative

nanosphere dimers at various separations, supplementary Figure 2, best-fit single exponential curves fit to the fractional shift in the surface plasmon resonance wavelength of two nanospheres as a function of the interparticle separation, supplemental Figure 3, DDA simulations of the optical extinction nanodisk dimers of three thicknesses at various separations and corresponding best-fit single exponential decays fit to the fractional surface plasmon resonance wavelength shift as a function of the interparticle separations scaled by the nanodisk diameter, supplemental Figure 4, DDA simulations of the optical extinction nanoprism dimers of three thicknesses at various separations and corresponding best-fit single exponential decays fit to the fractional surface plasmon resonance wavelength shift as a function of the interparticle separations scaled by the nanoprism bisector, and supplemental Figure 5, DDA simulations of the optical extinction nanocube dimers of three volumes at various separations and corresponding best-fit single exponential decays fit to the fractional surface plasmon resonance wavelength shift as a function of the interparticle separations scaled by the nanocube edge. This material is available free of charge via the Internet at http://pubs.acs.org.

References and Notes

(1) Kelly, K. L.; Coronado, E.; Zhao, L. L.; Schatz, G. C. *J. Phys. Chem. B* **2003**, *107*, 668–677.

(2) El-Sayed, M. A. *Acc. Chem. Res.* **2001**, *34*, 257–264.

(3) Link, S.; El-Sayed, M. A. *J. Phys. Chem. B* **1999**, *103*, 8410–8426.

(4) Bohren, C. F.; Huffman, D. R. *Absorption and Scattering of Light by Small Particles*; Wiley: New York, 1983.

(5) Choi, M.-R.; Stanton-Maxey, K. J.; Stanley, J. K.; Levin, C. S.; Bardhan, R.; Akin, D.; Badve, S.; Sturgis, J.; Robinson, J. P.; Bashir, R.; Halas, N. J.; Clare, S. E. *Nano Lett.* **2007**, *7*, 3759–3765.

(6) Gobin, A. M.; Lee, M. H.; Halas, N. J.; James, W. D.; Drezek, R. A.; West, J. L. *Nano Lett.* **2007**, *7*, 1929–1934.

(7) Huang, X.; El-Sayed, I. H.; Qian, W.; El-Sayed, M. A. *J. Am. Chem. Soc.* **2006**, *128*, 2115–2120.

(8) Huang, W.; Qian, W.; El-Sayed, M. A. *Adv. Mater. (Weinheim, Ger.)* **2008**, *20*, 733–737.

(9) Lin, A.; Boo, S.; Moon, D. S.; Jeong, H. J.; Chung, Y.; Han, W.-T. *Opt. Express* **2007**, *15*, 8603–8608.

(10) Maier, S. A.; Brongersma, M. L.; Kik, P. G.; Meltzer, S.; Requicha, A. A. G.; Atwater, H. A. *Adv. Mater. (Weinheim, Ger.)* **2001**, *13*, 1501–1505.

(11) Maier, S. A.; Kik, P. G.; Atwater, H. A.; Meltzer, S.; Harel, E.; Koel, B. E.; Requicha, A. A. G. *Nat. Mater.* **2003**, *2*, 229–232.

(12) Jiang, J.; Bosnick, K.; Maillard, M.; Brus, L. *J. Phys. Chem. B* **2003**, *107*, 9964–9972.

(13) Nikoobakht, B.; El-Sayed, M. A. *J. Phys. Chem. A* **2003**, *107*, 3372–3378.

(14) Willets, K. A.; Van Duyne, R. P. *Annu. Rev. Phys. Chem.* **2007**, *58*, 267–297.

(15) Zou, S.; Schatz, G. C. *Chem. Phys. Lett.* **2005**, *403*, 62–67.

(16) Rosi, N. L.; Mirkin, C. A. *Chem. Rev.* **2005**, *105*, 1547–1562.

(17) Rechberger, W.; Hohenau, A.; Leitner, A.; Krenn, J. R.; Lamprecht, B.; Aussenegg, F. R. *Opt. Commun.* **2003**, *220*, 137–141.

(18) Sweatlock, L. A.; Maier, S. A.; Atwater, H. A.; Penninkhof, J. J.; Polman, A. *Phys. Rev. B: Condens. Matter Mater. Phys.* **2005**, *71*, 235408/1–235408/7.

(19) Maier, S. A.; Brongersma, M. L.; Kik, P. G.; Atwater, H. A. *Phys. Rev. B: Condens. Matter Mater. Phys.* **2002**, *65*, 193408/1–193408/4.

(20) Jain, P. K.; Eustis, S.; El-Sayed, M. A. *J. Phys. Chem. B* **2006**, *110*, 18243–18253.

(21) Reinhard, B. M.; Siu, M.; Agarwal, H.; Alivisatos, A. P.; Liphardt, J. *Nano Lett.* **2005**, *5*, 2246–2252.

(22) Su, K. H.; Wei, Q. H.; Zhang, X.; Mock, J. J.; Smith, D. R.; Schultz, S. *Nano Lett.* **2003**, *3*, 1087–1090.

(23) Jain, P. K.; Huang, W.; El-Sayed, M. A. *Nano Lett.* **2007**, *7*, 2080–2088.

(24) Jain, P. K.; El-Sayed, M. A. *J. Phys. Chem. C* **2008**, *112*, 4954–4960.

(25) Jain, P. K.; El-Sayed, M. A. *J. Phys. Chem. C* **2007**, *111*, 17451–17454.

(26) Jain, P. K.; El-Sayed, M. A. *Nano Lett.* **2007**, *7*, 2854–2858.

(27) Gunnarsson, L.; Rindzevicius, T.; Prikulis, J.; Kasemo, B.; Kaell, M.; Zou, S.; Schatz, G. C. *J. Phys. Chem. B* **2005**, *109*, 1079–1087.

(28) Farinha, J. P. S.; Martinho, J. M. G. *J. Phys. Chem. C* **2008**, *112*, 10591–10601.

(29) Roy, R.; Hohng, S.; Ha, T. *Nat. Meth.* **2008**, *5*, 507–516.

(30) Fromm, D. P.; Sundaramurthy, A.; Schuck, P. J.; Kino, G.; Moerner, W. E. *Nano Lett.* **2004**, *4*, 957–961.

(31) Lee, C.-T.; Wang, M.; Jarnagin, N. D.; Gonsalves, K. E.; Roberts, J. M.; Wang, Y.; Henderson, C. L. *Proc. SPIE—Int. Soc. Opt. Eng.* **2007**, *6519*, 65191E/1–65191E/9.

(32) Flatau, P. J.; Stephens, G. L.; Draine, B. T. *J. Opt. Soc. Am. A: Opt., Image Sci., Vision* **1990**, *7*, 593–600.

(33) Goodman, J. J.; Draine, B. T.; Flatau, P. J. *Opt. Lett.* **1991**, *16*, 1198–200.

(34) Johnson, P. B.; Christy, R. W. *Phys. Rev. B: Solid State* **1972**, *6*, 4370–4379.

(35) Brioude, A.; Jiang, X. C.; Pileni, M. P. *J. Phys. Chem. B* **2005**, *109*, 13138–13142.

(36) Lee, K.-S.; El-Sayed, M. A. *J. Phys. Chem. B* **2005**, *109*, 20331–20338.

(37) Schatz, G. C. *THEOCHEM* **2001**, *573*, 73–80.

(38) Wiley, B. J.; Im, S. H.; Li, Z.-Y.; McLellan, J.; Siekkinen, A.; Xia, Y. *J. Phys. Chem. B* **2006**, *110*, 15666–15675.

(39) Boneberg, J.; Koenig-Birk, J.; Muenzer, H. J.; Leiderer, P.; Shuford, K. L.; Schatz, G. C. *Appl. Phys. A: Mater. Sci. Process.* **2007**, *89*, 299–303.

(40) Le, F.; Brandl, D. W.; Urzhumov, Y. A.; Wang, H.; Kundu, J.; Halas, N. J.; Aizpurua, J.; Nordlander, P. *ACS Nano* **2008**, *2*, 707–718.

(41) Jaeckel, F.; Kinkhabwala, A. A.; Moerner, W. E. *Chem. Phys. Lett.* **2007**, *446*, 339–343.

(42) Shuford, K. L.; Ratner, M. A.; Schatz, G. C. *J. Chem. Phys.* **2005**, *123*, 114713/1–114713/9.

(43) Hao, E.; Schatz, G. C. *J. Chem. Phys.* **2004**, *120*, 357–366.

JP807904S